
Interaction of DNA with a porphyrin ligand: evidence for intercalation

R.J.Fiel, J.C.Howard, E.H.Mark and N.Datta Gupta*

Department of Biophysics Research, Roswell Park Memorial Institute, Buffalo, NY 14263, and
*South Carolina State College, Orangeburg, SC 29115, USA

Received 2 April 1979

ABSTRACT

The porphyrin photosensitizer, meso-Tetra(4-N-methylpyridyl)porphine tetraperchlorate binds to calf thymus DNA by intercalation and by external electrostatic association. This was concluded from the results of measurements involving Scatchard analysis, viscometry, thermal denaturation, and circular dichroism.

INTRODUCTION

Several physical studies have shown that binding of polycyclic aromatic ligands to DNA can occur through at least two distinct modes. The binding mode of lowest free energy has been interpreted as intercalation (1-3). This is characterized by the interaction of the nucleotide bases with the planar ligand. The weaker binding mode is generally described as an electrostatic externally bound ligand, and is therefore characterized by a predominant interaction of the ligand molecules stacked along the external surface of the DNA.

X-ray crystallographic studies have provided direct evidence for intercalation (4,5); however, several other methods also have provided support for this model. For example, an enhanced stability of the intercalation complex has been noted by an increase in T_m (1). Viscosity and sedimentation measurements apparently reflect an increase in the chain length of DNA, which results from the insertion of the ligand (6). Circular dichroism studies have shown the existence of multimode binding to DNA, and measurements of very high affinity found for several planar ligands to DNA

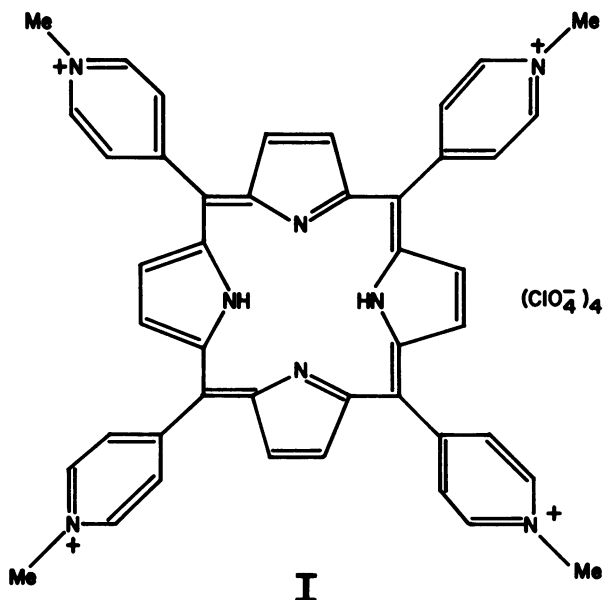
have all been interpreted as intercalation.

In the present investigation, we examined the interaction of meso-Tetra(4-N-methylpyridyl)porphine tetraperchlorate (T4MPyP) to DNA and found sufficient evidence which indicates that this porphyrin can bind by intercalation. We view this as a significant finding because of the ubiquitous roles found for natural porphyrins in normal physiological functions, as well as their potential as photodynamic and radiation sensitizers (7,8). Equally important is the potential relevance of this finding to the mechanism by which porphyrins induce photodynamic carcinogenesis (9).

Materials and Methods

Meso-Tetra(4-N-methylpyridyl)porphine tetraperchlorate (I) (M.W. 1076) was prepared as previously described (10). Aqueous solutions of calf thymus DNA (Worthington) were also prepared as previously described (11). All other materials were reagent grade.

All spectrophotometric measurements were done with a



Beckman model DB-G recording spectrophotometer. Ligand binding measurements were carried out using the spectrophotometric procedure described by Peacocke (2) and a Scatchard analysis (12). The extinction coefficient for T4MPyP in three different buffers, BPES (6 mM Na_2HPO_4 , 2 mM NaH_2PO_4 , 1 mM EDTA, 179 mM NaCl, pH6.8, $\mu = 0.196$), BPES with 1 M NaCl in place of 179 mM NaCl ($\mu = 1.017$), and BPES prepared without NaCl ($\mu = 0.017$). The values for the molar extinction coefficients were determined by least squares analysis of the absorbance versus concentration curves in each solution.

The molar extinction coefficient for porphyrin bound to DNA was determined in two ways. The absorbance at 424 nm was measured for solutions of DNA at a concentration of 3 mg/ml (4.5×10^{-3} M b.p.) in BPES buffer to which T4MPyP had been added over a concentration range of 1 to 8.5 $\mu\text{g/ml}$ (9.3 to 79.0×10^{-7} M). A linear plot was obtained with a correlation coefficient of 0.9999, and the molar extinction coefficient was determined to be $1.130 \times 10^5 \text{ M}^{-1} \text{ cm}^{-1}$. The second procedure was independent from the first, and the highest concentration of DNA used was 75 $\mu\text{g/ml}$. Measurements were made so that $(\epsilon_f - \epsilon_a)^{-1}$, the difference between the extinction coefficient of the free porphyrin and the apparent extinction coefficient of porphyrin in the presence of DNA, could be plotted against the reciprocal of the molar concentration of base-pairs. The linear portion of this curve was extrapolated to give the value of $(\epsilon_f - \epsilon_a)^{-1}$ at an infinite concentra-

Table 1

Molar Extinction Coefficients					
for the Visible Spectrum of 4TMPyP in BPES Buffer					
λ (nm)	424	520	555	585	650
$\epsilon \times 10^{-3}$	194	12.5	4.79	5.01	1.89

tion of base-pairs, i.e., the value for the extinction coefficient of the complex. This gave a value of $1.127 \times 10^5 \text{ M}^{-1} \text{ cm}^{-1}$ in excellent agreement with the value determined by the direct procedure. However, because of the limitations imposed upon these measurements by the instrument employed, we present our Scatchard analysis results with the reservation that it represents an order of magnitude of the binding constant.

Viscosity measurements were made at 25°C with Cannon-Ubbelohde semi-micro dilution viscometers and a Neslab PMT constant temperature bath. The ratios of the specific viscosity of DNA solutions with added porphyrin, relative to the specific viscosity of DNA solutions without porphyrin added, were plotted against P, the molar ratio of porphyrin to DNA base pairs.

Circular dichroism spectra were obtained using a Jasco-J41C spectropolarimeter. The 1 nm spectral bandwidth was controlled automatically. A Haake FK circulator was used to control the temperature in a water-jacketed 1.0 cm pathlength cylindrical quartz cell. The temperature of $25.0 \pm 0.3^\circ\text{C}$ in the cell was measured with a YSI #701 probe attached to a Digitec model 5810 thermometer. The concentrations of the samples are given in the appropriate figure legends.

Thermal denaturation data were obtained using a Gilford 2400-2 spectrophotometer equipped with an automatic reference compensator and cell selector. The temperature increase was controlled to $2/3^\circ\text{C}$ per minute using a Neslab TP-2 Programmer attached to a Haake FJ circulator.

RESULTS

A. Spectroscopy

The ultra-violet absorption spectra of DNA in figure 1 show a small hypochromic effect for the interaction with T4MPyP in BPES buffer. A maximum absorption band for free porphyrin appears at 262 nm and at 260 nm for DNA. Combined, these components show a maximum at 261 nm with approximately 11% hypochromicity.

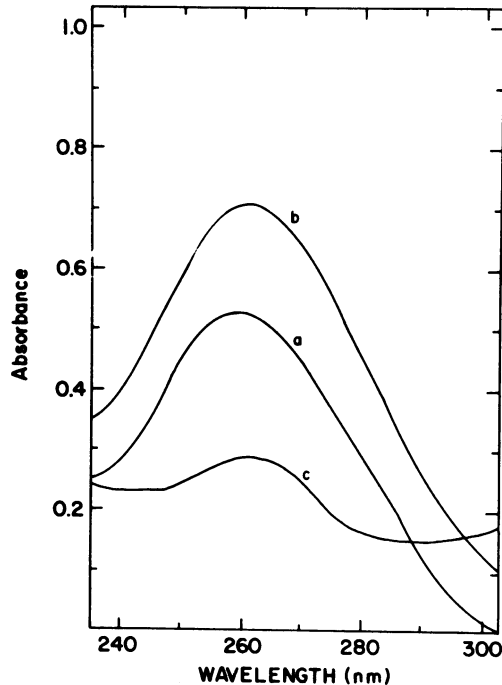


Figure 1. Absorption spectra of a. 3.79×10^{-5} M DNA (in base pairs) b. DNA plus T4MPyP at $P = 0.049$ c. 1.9×10^{-6} M T4MPyP, all in BPES buffer.

A greater effect can be seen in the visible region, as shown in figure 2, where the intensity of the Soret absorption at 424 nm decreases with an increasing concentration of DNA. In addition to a decrease of absorbance, a 4 nm shift of the maximum to a longer wavelength is observed. A single isobestic point was not observed for the range of concentration used.

The hypochromic effect noted in both the visible and ultra-violet regions is taken as evidence of an interaction between the DNA and porphyrin. This particular porphyrin is known not to self-stack up to 10^{-4} M according to Pasternack (11), based upon a correlation with Beer's law. We have confirmed this for concentrations up to 1.86×10^{-5} M in all three buffers used in this work, viz., BPES, BPES with 1 M NaCl and

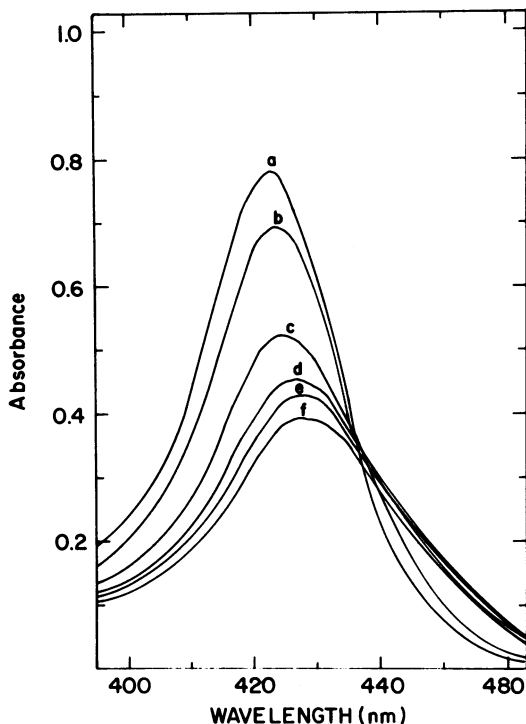


Figure 2. Absorbance spectra of a. 4.7×10^{-6} M T4MPyP b. T4MPyP plus DNA at P = 1.53 c. P = 0.511 d. P = 0.256 e. P = 0.153 f. P = 0.102.

BPES without NaCl. This does not exclude the possibility of an induced self-stacking as the result of binding to DNA phosphates at closely spaced intervals, which could account for the hypochromic effect noted in the Soret band. Another possibility is that the hypochromic effect is caused by the interaction of porphyrin molecules with the purine and pyrimidine bases of DNA via intercalation. It is also possible that the hypochromicity could be caused by some combination of the electrostatic and intercalation binding modes.

Before examining the mode of binding, it is informative to establish the degree of binding. This was accomplished using a Scatchard plot analysis of the spectrophotometric data

obtained by the method described by Peacocke (2). A typical Scatchard analysis of the binding of T4MPyP to DNA is shown in figure 3 as a plot of r/m versus r . The letter r represents the number of moles of porphyrin bound/mole of DNA base pairs, and m is the concentration of unbound porphyrin. The general shape of the curve is indicative of complex binding, which may be treated using a number of available models (14). Evidence to be presented from our circular dichroism and melting profile experiments suggests that two binding sites or binding modes are involved at the moderate ionic strength of BPES buffer. The first and stronger binding is characterized as intercalation has been analyzed from the linear portion of the Scatchard plot at small values of r . A value of 1.10×10^7 was determined for k , the binding constant, and 0.14 for n , the number of moles of porphyrin bound per mole of base pairs.

The weaker binding can be characterized as an external association of the porphyrin with the phosphate groups of DNA.

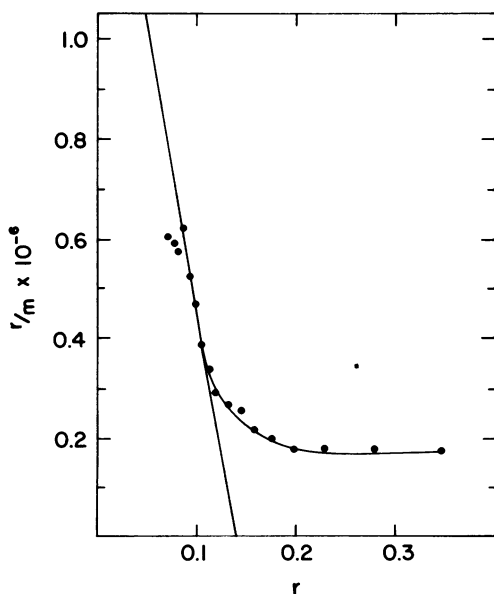


Figure 3. Scatchard plot of the binding of T4MPyP to calf thymus DNA in BPES buffer.

An interesting example of this relatively weak electrostatic binding is shown in figure 4, where ϵ_a , the apparent molar extinction coefficient of T4MPyP in the presence of a copolymer of divinyl ether/maleic anhydride, is plotted versus the molar (monomer) concentration of the copolymer. For comparison, a corresponding plot of T4MPyP in the presence of DNA is also shown. In the case of the copolymer, which is usually referred to as Pyran copolymer, ϵ_a remains nearly constant in 1 M NaCl for a molar concentration of Pyran monomer up to 30×10^{-6} . In this case, there is adequate counterion present to shield any interaction between T4MPyP and the carboxylate groups of Pyran. The small decrease of ϵ_a noted in BPES buffer indicates a small degree of binding of the porphyrin to Pyran. This can be compared to the lower curve, illustrating

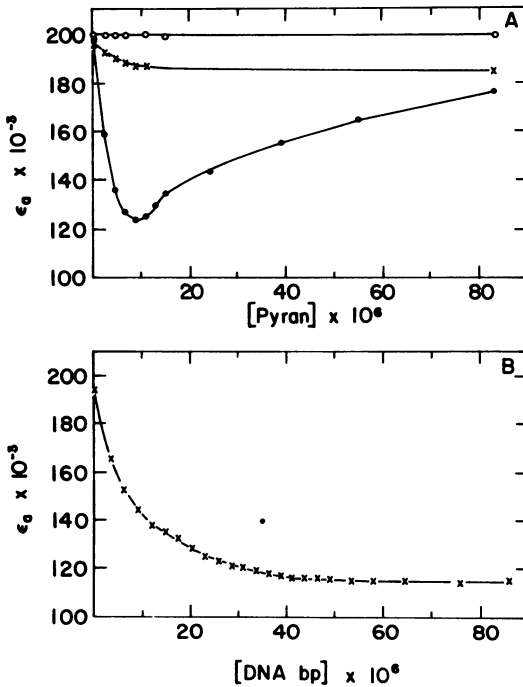


Figure 4. A. Apparent molar extinction coefficient at $\lambda = 424 \text{ nm}$ for T4MPyP in Pyran copolymer in o. BPES buffer - NaCl, x BPES buffer o. BPES buffer with 1M NaCl. B. Apparent molar extinction coefficient at $\lambda = 424 \text{ nm}$ for T4MPyP in calf thymus DNA in BPES buffer.

the effect on ϵ_a of the binding of T4MPyP to DNA. Considering that these two polymers, DNA and Pyran, have approximately the same charge density,¹ it is apparent that electrostatic binding alone cannot account for the large decrease of ϵ_a in the case of DNA.

The final Pyran curve shows the change of ϵ_a in BPES buffer prepared without NaCl. In the absence of Na⁺ counterion, a strong electrostatic interaction is possible resulting in a high degree of binding. This is reflected by a steep decrease in ϵ_a to a minimum which corresponds to a ratio of approximately 1 porphyrin molecule/2 monomer units (8 carboxylate groups). As the Pyran concentration increases, ϵ_a begins to increase to the value of the molar extinction for the free porphyrin ϵ_f . In the case of DNA, ϵ_a appears to level-off at a value which is considerably less than ϵ_f .

B. Viscometry

Additional information regarding the nature of porphyrin binding has been obtained from viscosity measurements. The effect of the addition of T4MPyP to a solution of DNA on its viscosity is shown in figure 5. Although the increase of viscosity is small, it correlates with the known effect of intercalation found for other DNA-dye interactions (1). This result, when coupled with the strong binding and complex Scatchard plot observed for T4MPyP, suggests that intercalation may be an important mode of binding for this particular porphyrin.

C. Thermal Denaturation/Absorbance-Temperature Transition Profiles

The melting profile of DNA also is sensitive to the addition of T4MPyP as shown in figure 6. The upper curve, the DNA control in BPES buffer, has a T_m of 91.4°C. Addition of 2 $\mu\text{g/ml}$ ($1.9 \times 10^{-6}\text{M}$) of T4MPyP to 25 $\mu\text{g/ml}$ ($3.8 \times 10^{-5}\text{M}$ b.p.) of DNA ($P = 0.049$, the input ratio of the moles of porphyrin to moles of base pairs) increases the T_m to 93.7°C and lowers the hyperchromicity, H_{260} , to approximately 28%. This reflects

¹ The calculated linear charge density, ξ , for Pyran was found to be 3.7, compared to the value of 4.2 for DNA (15).

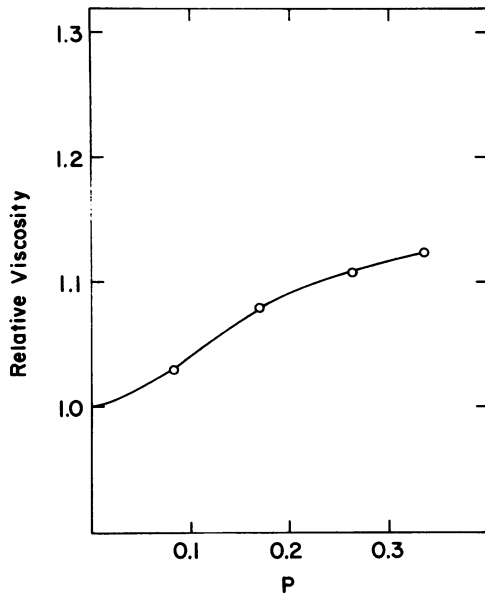


Figure 5. Relative viscosity of calf thymus DNA in BPES buffer as a function of the concentration of added T4MPyP.

a stabilization of the double helix. Additional evidence, presented in table 2, shows the effect of increasing P on the T_m . The apparent trend shows a direct relationship between the ratio P, and an increasing stabilization effect on the T_m .

Another approach is to measure the absorbance-temperature transition profile by monitoring the Soret band, i.e., H_{424} . Since the absorbance of the porphyrin decreases on binding to DNA, a decrease in binding, as a result of heat or other treatment, should increase the absorbance. This has been shown to be the case and has proven to be useful in establishing binding modes, as indicated in figure 7. The control curve, DNA-free porphyrin, shows a slight decrease of absorbance with increasing temperature. This can be attributed to a decrease in concentration that accompanies the thermal expansion of the solution. The absorbance recovers to its initial value when the solution is cooled to room temperature.

In the presence of 2.27×10^{-5} M DNA base pairs, a bimodal

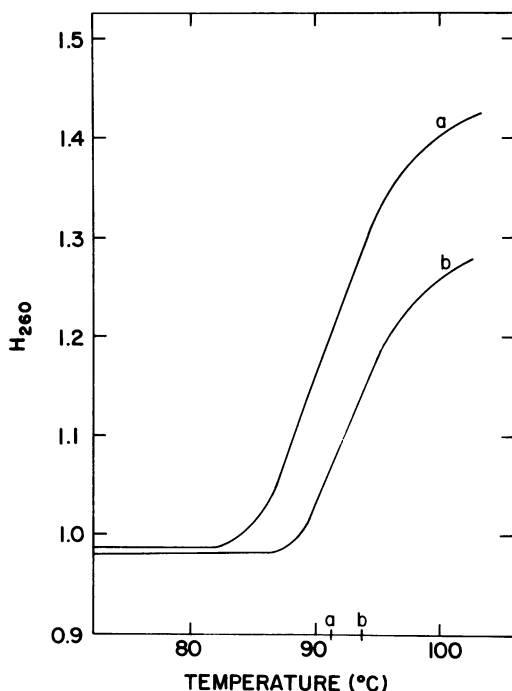


Figure 6. Hyperchromicity - temperature profile at 260 nm for
 a. DNA in BPES buffer b. DNA plus T4MPyP at $P = 0.049$.

thermal transition curve is obtained for the porphyrin absorbance. The transition curve is composed of two hyperchromic steps separated from each other by a point corresponding to the DNA T_m . As the concentration of DNA is increased, H_{424} increases as well, and the point between the two transitions becomes a minimum in the transition profile. This is further demonstrated in figure 8 for concentrations of DNA up to $45.4 \times 10^{-5} M$. The initial increase in absorbance, extending from 25° to approximately $70^\circ C$, reflects the thermal barrier to the weak electrostatic interaction between the cationic charge of the porphyrin and the DNA backbone phosphates and the subsequent porphyrin-porphyrin interaction. The first maximum at approximately 70° corresponds to the start of the melting of DNA. From this point, the absorbance begins to decrease to a

Table 2

Melting Temperature and Hyperchromicity of DNA/ Porphyrin Solutions in BPES and BPES (-NaCl) Buffer		
<u>P*</u>	<u>T_m</u>	<u>H</u>
control (BPES)	91.4	42.5
0.031	92.0	39.6
0.049	93.7	28.0
0.061	94.0	34.5
0.088	95.0	35.0
0.184	96.7	30.0
control (-NaCl)	71.0	44.0
0.102	78.5	33.0
0.153	84.0	27.0

*P = input ratio of moles of 4TMPyP/moles nucleotide base pairs.

minimum which corresponds to the DNA T_m . At this point, the absorbance increases sharply as DNA completes its melting. Upon cooling to room temperature, H_{424} decreases smoothly in a one step process until it is approximately -20%.

At lower ionic strength, i.e., BPES buffer without NaCl, the effect is even more evident, as shown in figure 9. The first hyperchromic step is most apparent at the smallest porphyrin/DNA ratio. The electrostatic nature of this low temperature transition is also suggested by the results of absorbance-temperature transition measurements in BPES buffer

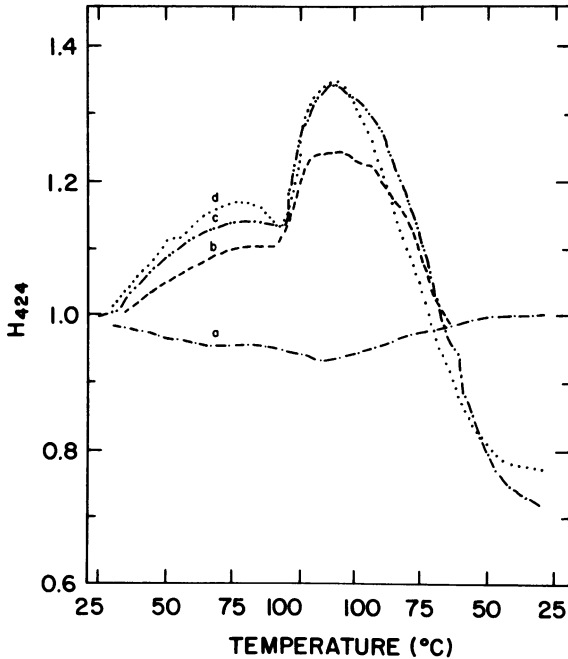


Figure 7. Hyperchromicity - temperature profile at 424 nm for 4TMPyP and DNA a. control 4.6×10^{-6} M T4MPyP b. P = 0.204 c. P = 0.123 d. P = 0.061. All in BPES buffer.

containing 1 M NaCl. Complete melting of DNA could not be obtained in this case because of the high ionic strength of the buffer. The most important feature of these experiments, however, is that the low temperature transition is absent, probably because of counterion shielding of any electrostatic interactions.

Another interesting feature of these melting curves is that, upon cooling to room temperature, the absorbance values for each sample at all three salt concentrations were found to be hypochromic relative to their initial values. Moreover, this hypochromicity was found to increase with an increasing concentration of salt. Compare, for example, figures 8, 9 and 10. The relationship of this effect to the molar ratio of porphyrin to DNA is shown in table 3. The hypochromicity was less sensitive to P when the medium or low ionic strength

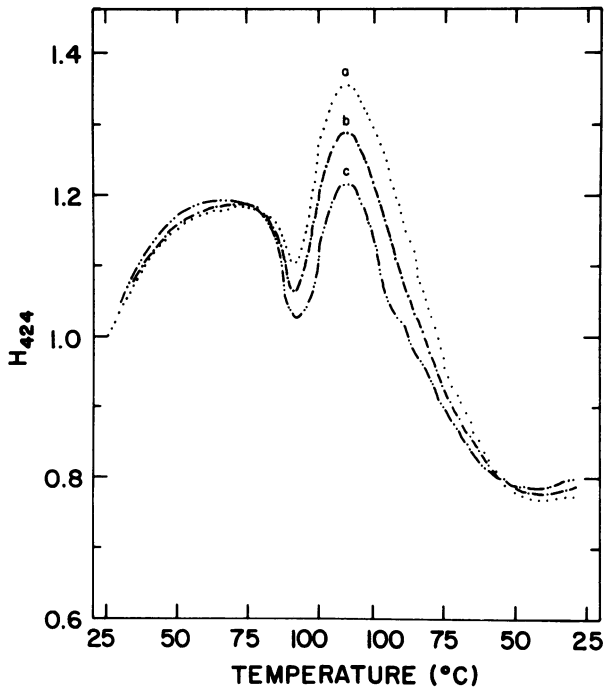


Figure 8. Hyperchromicity - temperature profile at 424 nm for T4MPyP and DNA at $P =$ a. 0.031 b. 0.016 c. 0.008. All in BPES buffer.

buffer was used; however, in high salt buffer the hyperchromicity was greatest at small values for P . A general conclusion made from the data in table 3 is that T4MPyP binds to denatured DNA to a greater extent than to native DNA.

D. Circular Dichroism

Circular dichroism spectra were recorded in both the ultraviolet and visible regions at various values of P . The CD spectrum of a solution of DNA and porphyrin, $P = 0.049$, is compared to the spectrum of a solution of an equivalent concentration of DNA in figure 11. The typical DNA spectrum has a negative and positive band at 247 and 278 nm, respectively, with approximately the same amplitude. Upon addition of T4MPyP, the amplitude of both bands decreases and the positive band 278 nm splits into a band at 284 nm and one at 268 nm.

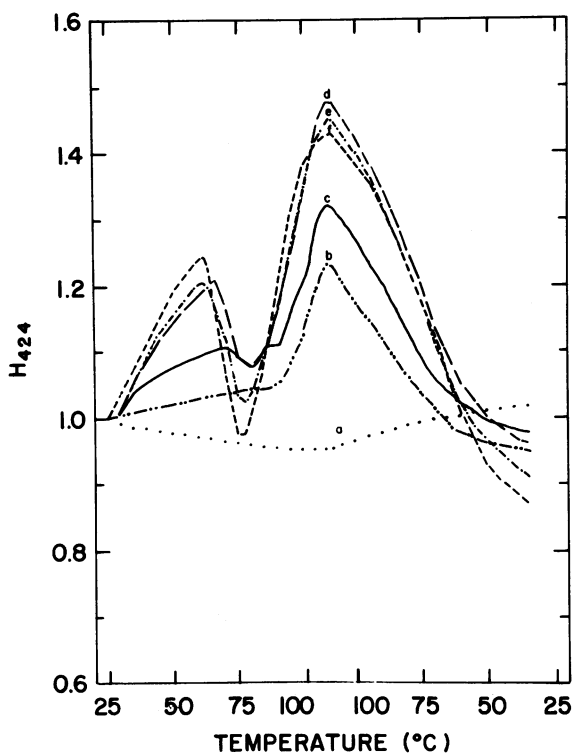


Figure 9. Hyperchromicity - temperature profile at 424 nm for T4MPyP and DNA a. control 4.6×10^{-6} M T4MPyP b. $P = 0.306$ c. $P = 0.153$ d. $P = 0.102$ e. $P = 0.061$ f. $P = 0.031$. All in BPES - NaCl buffer.

The spectrum now takes on the appearance of that of DNA in chromatin and suggests that a structural change has taken place. Since T4MPyP also has some absorption in this region, it must also be considered that the changes are the result of an induced CD signal of DNA bound porphyrin. Free T4MPyP does not exhibit a detectable signal in either the ultraviolet or visible region.

Circular dichroism activity is definitely induced in the visible region on binding T4MPyP to DNA. This is shown in figure 12 for $P = 0.184$. A strong positive band is apparent

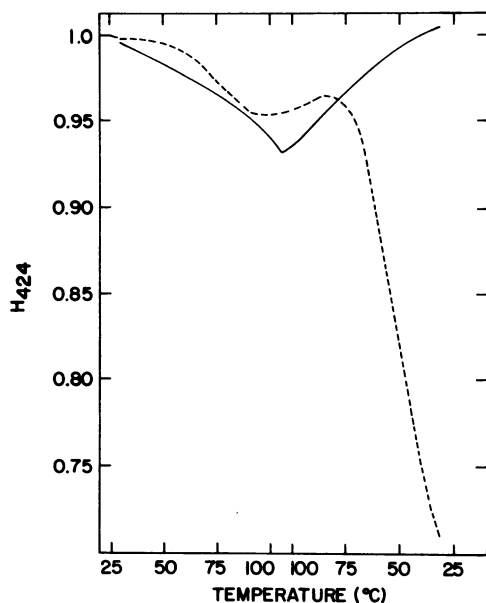


Figure 10. Hyperchromicity - temperature profile at 424 nm for T4MPyP and DNA. — control 4.6×10^{-6} M T4MPyP. --- P = 0.061. —. Both in BPES buffer with 1M NaCl.

at 417 nm and a slightly stronger negative band at 442 nm.¹

The cross over point corresponds to the Soret absorption for T4MPyP in BPES buffer. The interesting question is whether the two CD bands are characteristic of two different binding modes. This question was resolved in two ways. First, the variation in the amplitude of each band was measured as a function of P in BPES buffer, as shown in figure 13. Whereas, the amplitude of the negative band is apparently independent of P, the amplitude of the positive band is inversely proportional to P. Therefore, the positive band must result primarily from a porphyrin-base interaction that increases as the concentra-

¹ It should be noted that $\Delta\epsilon$ was calculated on the basis of the molar concentration of DNA base pairs in figure 11, whereas, in figure 12 and all other CD spectra of the visible region, $\Delta\epsilon$ was calculated on the basis of the input concentration of T4MPyP. This does not differentiate between the bound and unbound porphyrin.

Table 3

Final Hyperchromicity After Heating and Cooling.*			
<u>P</u>	BPES (1M NaCl)	<u>BPES</u>	BPES (-NaCl)
0.613	0.930	0.871	-
0.306	0.875	-	0.940
0.204	-	0.700	-
0.153	0.791	-	0.970
0.123	0.784	0.730	-
0.102	0.730	-	0.942
0.090	-	0.790	-
0.0613	0.708	0.789	0.887
0.0306	0.654	0.777	0.843
0.0153	0.604	0.787	-
0.0077	0.630	0.805	-

*A smaller value means a larger hypochromic effect.

tion of DNA increases. A differential dependence of these two bands upon the ionic strength of the buffer is shown in figures 14 and 15. The positive band increases with decreasing P, while the negative band is absent in 1 M NaCl. This suggests that the negative band is primarily the result of an electrostatic association with DNA that allows porphyrin-porphyrin interaction, and that this interaction is blocked by the high concentration of counterion. This is supported by the series of CD spectra shown in figure 15, measured in BPES buffer without NaCl, a condition that promotes electrostatic interaction between T4MPyP and DNA. Although the positive band is quite apparent, it is generally less intense

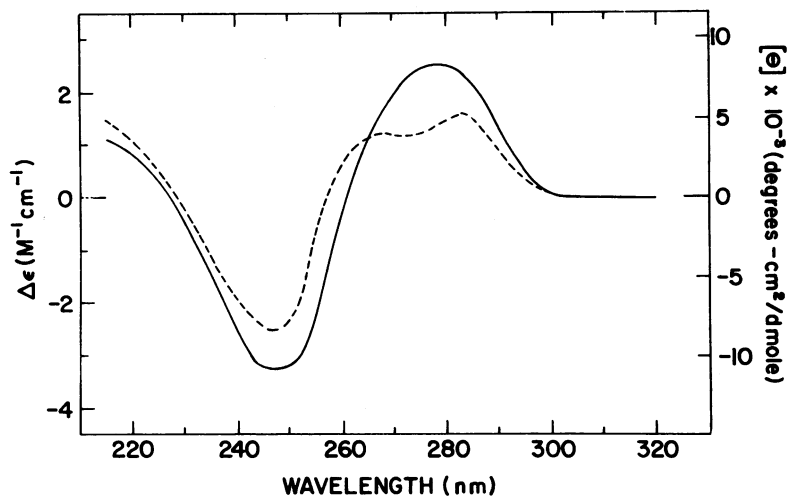


Figure 11. Circular dichroism spectra of DNA _____, and DNA plus T4MPyP -----, $P = 0.049$ in BPES buffer. $[DNA] = 3.8 \times 10^{-5}$

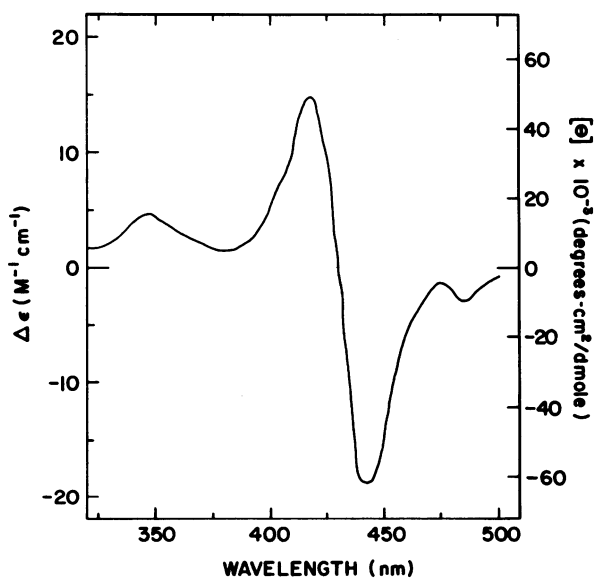


Figure 12. Circular dichroism spectra of T4MPyP and DNA at $P = 0.184$, in BPES buffer. $[T4MPyP] = 2.8 \times 10^{-6}$

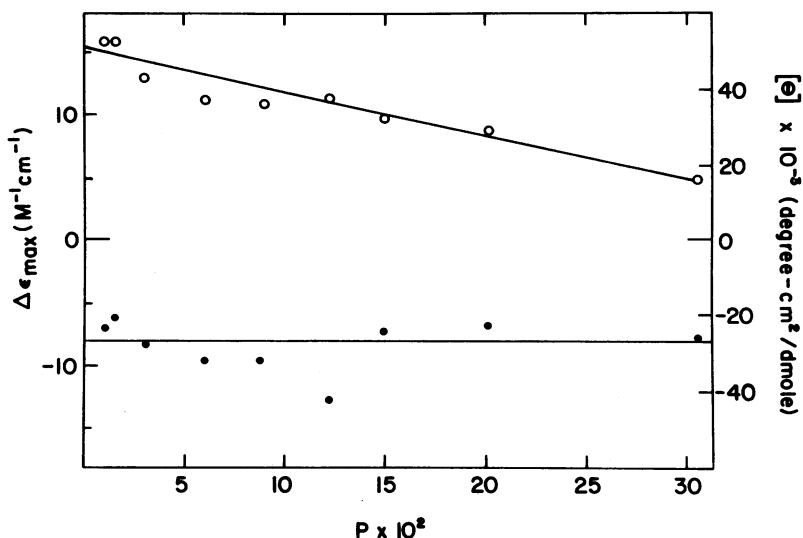


Figure 13. Change in $\Delta \epsilon_{\max}$ for the positive and negative CD bands as a function of P , in BPES buffer. $[T4MPyP] = 4.6 \times 10^{-6}$

than the corresponding negative band. Moreover, the negative band appears to increase as P increases, as expected for a porphyrin-porphyrin interaction.

Additional support for the assignment of the negative band primarily to electrostatically bound porphyrin can be seen from the thermal - CD experiment shown in figure 16. In this experiment, the amplitude of the negative band was followed throughout a heating-cooling cycle in low salt BPES. This can be compared with the T_m measurements in the same buffer shown in figure 9. In the CD measurement of figure 16, the amplitude of the negative band is seen to decrease to a minimum value as the temperature increases to approximately 60°C . This corresponds to the first maximum of the hyperchromicity curve in figure 9. As the temperature continues to increase, the amplitude of the CD band increases to a maximum at a temperature corresponding to the T_m . The amplitude then begins to decrease as DNA continues to denature. Upon cooling to room temperature, the amplitude increases to a value larger than its original value, thus, correlating with the effect noted

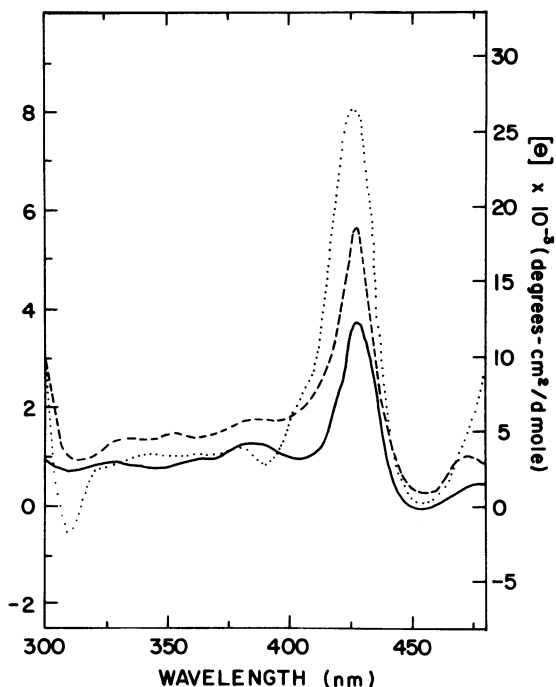


Figure 14. Circular dichroism spectra of T4MPyP and DNA at $P = 0.061$ ———, $P = 0.031$ -----, $P = 0.013$, All in BPES buffer with 1M NaCl. $[T4MPyP] = 4.6 \times 10^{-6}$

in the absorbance-temperature transition measurements.

DISCUSSION

Concluding that a particular compound binds to DNA by intercalation usually indicates that its properties are known to be similar to those of established intercalating agents, such as, ethidium bromide (14) or proflavine (2). On this basis, as is evident from the results already presented, we have concluded that T4MPyP can be classified as an intercalating agent.

The primary evidence that prompted this conclusion consists of four major points. The first is the hypochromic effect found for the major visible absorption band of the porphyrin upon binding to DNA. This does not dictate inter-

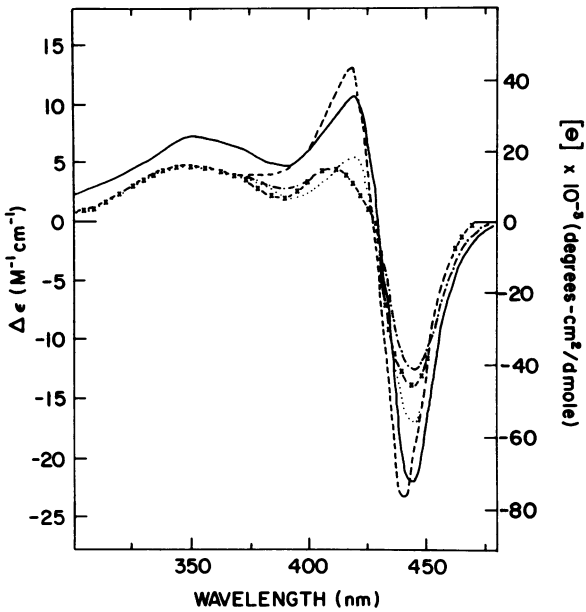


Figure 15. Circular dichroism spectra of T4MPyP and DNA at $P = 0.306$ ----, 0.153 _____, 0.102 , 0.061 -x-x-x-, 0.031 -·-·-·-, all in BPES buffer - NaCl. $[T4MPyP] = 4.6 \times 10^{-6}$

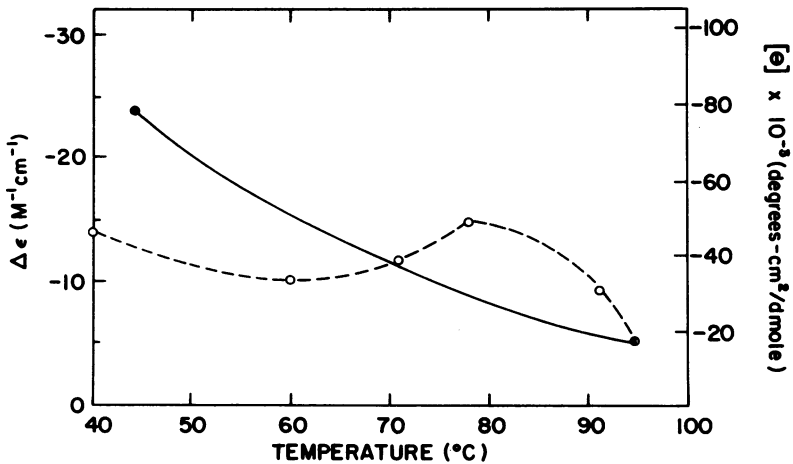


Figure 16. Temperature dependence of the negative CD band for T4MPyP and DNA at $P = 0.103$ in BPES buffer - NaCl. $[T4MPyP] = 4.6 \times 10^{-6}$

calative binding but only that binding, in which either porphyrin-porphyrin or porphyrin-base interaction, or both, has occurred. It is important to note, however, that in the case of T4MPyP the hypochromic effect was found to be substantial even at high ionic strength, where electrostatic interactions are blocked or at least minimized. In comparison, methyl green, a non-intercalating dye that can bind to DNA electrostatically, is displaced from DNA by 0.15 M NaCl (16).

The second point is that the binding constant determined for T4MPyP in BPES is equal to or larger than the binding constants found for a series of actinomycin intercalating agents in the same buffer (3). A comparison can also be made of the apparent number of binding sites, found to be 0.14 per base pair for T4MPyP, which correlates within the range of values, 0.08-0.2, found for the series of actinomycins (3).

Thirdly, viscosity and/or sedimentation measurements have often been used to establish the intercalating nature of a specific compound. Cohen and Eisenberg (6) carried out an extensive investigation of the viscosity and sedimentation characteristics of sonicated DNA-proflavine complexes. They concluded that their results were compatible with the intercalation model of Lerman (1). Although the increase in viscosity found for the DNA-porphyrin complex in the present work was relatively small, it is consistent with the Lerman model. The small effect may be that the increase was offset somewhat by the large cationic charge of the porphyrin.

Finally, the increase in the stability of the DNA double helix, as measured by an increase of the T_m , is also consistent with intercalation. It must be noted, however, that the relationship between the mode of binding of specific compounds to DNA and the T_m is a complex one. For example, methyl green, the aforementioned non-intercalating dye, increases the T_m of DNA (16) as does the diamino steroid series derived from diaminoandrostane (17). Consequently, the T_m results alone do not constitute evidence for intercalation; however, the sum of these four points supports the conclusion.

Besides this primary evidence, additional and more detailed knowledge of the mode(s) of binding of T4MPyP to

DNA has been obtained from measurements of the hyperchromicity of the visible spectrum and circular dichroism studies. Perhaps the most interesting result is the bimodal nature of the hyperchromicity in the absorbance-temperature transition measurements (figures 7-9). Two distinct transition zones are apparent in figure 7, which we attribute to the two modes by which the porphyrin is bound to DNA. The low temperature transition represents a weak electrostatic binding and the high temperature transition represents intercalative binding. This interpretation is supported by the results shown in figure 10, where the low temperature transition has been blocked by a high concentration of counterions, and by the increased predominance of the low temperature transition found at very low ionic strength, shown in figure 9.

Two additional observations should also be noted from these results. The first is that the transition profiles are more accurately characterized as trimodal transitions in most instances. This description takes into account the decrease in absorbance that generally follows the low temperature transition and precedes the high temperature transition. This decrease appears to result from a new binding process in which the porphyrin interacts with base residues exposed as the DNA enters a pre-melting or partially denatured phase. It is most apparent at low ionic strength and small P. This may reflect insertion of the porphyrin into "kinks" (18) formed as part of a pre-melting process.

The second point refers to the final absorbance value attained by the porphyrin-DNA complexes upon cooling to room temperature. In all cases, these values tend to be lower than the initial values obtained upon mixing the two components, DNA and porphyrin (figures 7-10). This indicates an increase in binding of T4MPyP to denatured DNA. Moreover, this binding appears to be favored by high ionic strength, as indicated in figure 10, and may therefore differ from that observed by the absorbance decrease during the heating portion of the cycle.

The circular dichroism studies have been particularly useful in the visible region where measurements are free from interference from DNA. Although DNA-free solutions of T4MPyP

show no circular dichroism, binding of the porphyrin to DNA clearly induces a strong signal. In an effort to determine the nature of the porphyrin binding, the effects of three variables on the CD spectra of porphyrin-DNA complexes were studied.

The first was to measure the CD spectrum as a function of P. An interaction between the porphyrin and DNA bases would be favored by a decrease in the intensity of the signal as P is increased. This was found to be the case for the positive band at 417 nm (figure 12) as shown in figure 13. The negative band at 442 nm was found to be unchanged up to P = 30.

The second variable studied was the ionic strength. Here it was noted that in the presence of 1 M NaCl, the negative band could not be observed up to P = 0.061, whereas, the positive band, although shifted to 428 nm, had the same characteristics as in the previous experiment (figure 14). At low ionic strength (figure 15), the negative band predominates at all values of P. These data are consistent with a model in which the positive band represents primarily base-porphyrin interaction that is increased as the ionic strength is increased. The negative band represents primarily porphyrin-porphyrin interaction that depends upon electrostatic binding of the porphyrin with DNA, and is consequently easily eliminated at a high counterion concentration.

It should be noted that these empirical assignments are not necessarily meant to reflect an absolute separation of the spectral response of the two binding modes. We recognize that these bands may contain some overlap and/or long range, ca. 25Å, coupling of the transition moments of intercalated porphyrin with externally bound porphyrin. A final resolution of this problem will require correlation between calculated and observed spectra.

The temperature dependence of the negative CD band was followed as the third and final variable to be measured. This was carried out at low ionic strength, as shown in figure 16, where the electrostatic interaction is apparently quite strong. The profile shown in figure 16, showing a decrease of intensity at the beginning of the heating cycle followed by an increase

and a second decrease, correlates with the temperature absorbance-transition measurements (figures 7-10). That portion of the porphyrin which is associated with the phosphate groups of DNA is dissociated at a relatively low temperature, and the intensity of the CD band correspondingly decreases. At the point at which the absorbance in the absorbance-temperature transition profile begins to decrease, the intensity of the CD band begins to increase, both changes reflecting increased binding. When the melting temperature of the DNA is reached, the CD signal begins to decrease and the absorbance increases. Finally, when cooled to room temperature, a very intense CD band is observed. This is compatible with our previous observation that T4MPyP may bind more to denatured than to native DNA. This may also reflect a higher molar extinction coefficient for the bound species of the former case.

In summary, we believe that the sum of these data strongly suggests that T4MPyP binds to DNA in two and possibly three ways. The first is electrostatic binding between the cationic charge of the porphyrin and the DNA backbone phosphates. The second is an intercalation of the porphyrin between DNA base pairs. The third mode requires partially or fully denatured DNA and involves a porphyrin-base interaction.

Our observation of the ability of T4MPyP to intercalate into DNA is the first time this has been shown for a porphyrin. It should be noted that T4MPyP is too bulky to intercalate without rupturing hydrogen bonds between DNA base-pairs and distorting the double helix. Intercalation of T4MPyP may therefore reflect the existence of DNA "breathing" (18-20). Because of the importance of this observation, it is essential that the binding of T4MPyP to DNA be investigated using other techniques. Unwinding of covalently closed supercoiled DNA is generally considered to be an important characteristic of intercalating agents. T4MPyP has been shown to unwind Col E1 DNA (21). The high charge density of T4MPyP does, however, impart to it some unique characteristics, which will be described in that work (21). Additional significance of this finding rests with its potential relationship to photochemotherapy as well as photodynamic carcinogenesis.

ACKNOWLEDGEMENTS

This work was supported in part by NIH-DRR-RR-08060-06 and NIH-ES-07057-01.

The authors thank Drs. Robert Woody and Allen Bush for helpful discussions.

REFERENCES

1. Lerman, L. S. (1964) *J. Cell Comp. Physiol.* 64 Sup. 1, 1-18.
2. Peacocke, A. R. and Skerrett, J. N. H. (1956) *Trans. Faraday Soc.* 52, 261-279.
3. Muller, W. and Crothers, D. M. (1968) *J. Mol. Biol.* 35, 251-290.
4. Tsai, C. C., Jain, S. C. and Sobell, H. M. (1977) *J. Mol. Biol.* 114, 333-365.
5. Sakore, T. D., Jain, S. C., Tsai, C. C. and Sobell, H. M. (1977) *Proc. Natl. Acad. Sci.* 74, 188-192.
6. Cohen, G. and Eisenberg, H. (1969) *Biopolymers* 8, 45-55.
7. Dougherty, T. J., Grindey, G. B., Fiel, R., Weishaupt, K. R. and Boyle, D. G. (1975) *J. Natl. Cancer Inst.* 55, 115-119.
8. Fiel, R. J., Mark, E. H. and Datta Gupta, N. (1975) *Res. Comm. Chem. Path. Pharm.* 10, 65-76.
9. Bungeler, W. (1937) *Z. Krebsforsch.* 46, 130-167.
10. Datta Gupta, N., Fanning, J. C. and Dickens, L. L. (1976) *J. Coord. Chem.* 5, 201-207.
11. Levine, H. I., Fiel, R. J. and Billmeyer, F. W., Jr. (1976) *Biopolymers* 15, 1267-1281.
12. Scatchard, G. (1949) *Ann. N. Y. Acad. Sci.* 51, 660-672.
13. Pasternack, R. F. (1973) *Ann. N. Y. Acad. Sci.* 206, 614-630.
14. Bontemps, J. and Fredericq, E. (1974) *Biophys. Chem.* 2, 1-22.
15. Anderson, C. F. and Record, M. T., Jr. (1978) *Biophys. Chem.* 7, 301-316.
16. Krey, A. K. and Hahn, F. E. (1975) *Biochem.* 14, 5061-5067.
17. Waring, M. J. and Henley, S. M. (1975) *Nucleic Acids Res.* 2, 567-586.
18. Sobell, H. M., Reddy, B. S., Bhandary, K. K., Jain, S. C., Sakore, T. D. and Seshadri, T. P. (1977) *Cold Springs Harbor Sym.* 42, 87-102.
19. Li, H. J. and Crothers, D. M. (1969) *J. Mol. Biol.* 39, 461-477.
20. McGhee, J. D. and von Hippel, P. H. (1975) *Biochem.* 14, 1281-1296.
21. Fiel, R. J. and Munson, B. R., Manuscript in preparation.